Glycobiology, 2017, vol. 27, no. 1, 87–98
doi: 10.1093/glycob/cww078
Advance Access Publication Date: 13 September 2016
Original Article

OXFORD

Glycan Synthesis

Cryptococcus neoformans UGT1 encodes a UDP-Galactose/UDP-GalNAc transporter

Lucy X Li[2], Angel Ashikov[3,4], Hong Liu[2,5], Cara L Griffith[2,5], Hans Bakker[3], and Tamara L Doering[2,1]

[2]Department of Molecular Microbiology, Washington University School of Medicine, St. Louis, MO, 63110, USA and [3]Department of Cellular Chemistry, Hannover Medical School, D-30625 Hannover, Germany

[1]To whom correspondence should be addressed: Tel: +1-314-362-2761; Fax: +1-314-362-1232; e-mail: doering@wustl.edu

[4]Present address: Department of Neurology, Radboud University Nijmegen Medical Centre, Nijmegen, The Netherlands.

[5]Present address: Monsanto Corporation, St. Louis, MO, 63167, USA.

Received 27 May 2016; Revised 22 July 2016; Accepted 27 July 2016

Abstract

Cryptococcus neoformans, an opportunistic fungal pathogen, produces a glycan capsule to evade the immune system during infection. This definitive virulence factor is composed mainly of complex polysaccharides, which are made in the secretory pathway by reactions that utilize activated nucleotide sugar precursors. Although the pathways that synthesize these precursors are known, the identity and the regulation of the nucleotide sugar transporters (NSTs) responsible for importing them into luminal organelles remain elusive. The UDP-galactose transporter, Ugt1, was initially identified by homology to known UGTs and glycan composition analysis of *ugt1*Δ mutants. However, sequence is an unreliable predictor of NST substrate specificity, cells may express multiple NSTs with overlapping specificities, and NSTs may transport multiple substrates. Determining NST activity thus requires biochemical demonstration of function. We showed that Ugt1 transports both UDP-galactose and UDP-*N*-acetylgalactosamine in vitro. Deletion of *UGT1* resulted in growth and mating defects along with altered capsule and cellular morphology. The mutant was also phagocytosed more readily by macrophages than wild-type cells and cleared more quickly in vivo and in vitro, suggesting a mechanism for the lack of virulence observed in mouse models of infection.

Key words: *Cryptococcus neoformans*, nucleotide sugar transporters, polysaccharide capsule, UDP-galactose, UDP-GalNAc

Introduction

Cryptococcus neoformans is an opportunistic fungal pathogen that is ubiquitous in the environment. It infects over a million people worldwide each year and kills over 600,000 of them, disproportionately affecting resource-limited areas (Park et al. 2009). Cryptococcosis is initially acquired by inhalation of fungal cells or spores into the lower respiratory tract (Botts and Hull 2010). This leads to a primary pulmonary infection, which is normally controlled by alveolar macrophages. In immunocompromised individuals, however, fungi can proliferate and disseminate throughout the host, with a particular tropism for the brain.

The principal virulence factor of *C. neoformans* is a polysaccharide capsule, which helps it evade the host immune response. This structure surrounds the yeast cell wall, which as in other fungi is made of glucans, chitin, and mannoproteins (Doering 2009). The capsule is composed of two polysaccharides, glucuronoxylomannan (GXM) and glucuronoxylomannogalactan (GXMGal), with trace amounts of mannoproteins (Kumar et al. 2011). These polymers, which are synthesized intracellularly (Yoneda and Doering 2006), become associated with the outer surface of the cryptococcal cell wall (Reese et al. 2007), forming a protective layer that impedes phagocytosis and immune mediator binding (Voelz and May 2010).

This structure is highly responsive to environmental conditions, becoming particularly large during infection of mammalian hosts (Doering 2009). Capsule polysaccharides are also continually shed from the yeast, and act in suppression of the host immune response (Voelz and May 2010). Understanding the pathways that produce the capsule and other essential glycoconjugates is central to developing strategies to effectively disrupt their function and combat this lethal pathogen.

GXM typically constitutes ~90% of the capsule mass (Doering 2009). It is a repeating polymer, made up of a mannose backbone with glucuronic acid (GlcA) and xylose (Xyl) side chains (Cherniak et al. 1998) (all sugars are pyranose forms unless otherwise indicated). GXMGal, which makes up the remaining 10% of the capsule mass, consists of a galactan backbone modified with galactomannan side chains bearing a variable number of Xyl and GlcA residues (Heiss et al. 2009); the backbone may also be modified with single galactofuranose (Gal_f) residues (Heiss et al. 2013). Mutants lacking either or both capsular polysaccharides are avirulent (Chang and Kwon-Chung 1994; Moyrand et al. 2007).

C. neoformans dedicates a significant portion of its genetic machinery and metabolic energy to synthesizing capsule and other cellular glycoconjugates, including protein-linked glycans (Olson et al. 2007; Reilly et al. 2011; Park et al. 2012), cell wall components (Reese and Doering 2003; Banks et al. 2005; Reese et al. 2007; Gilbert et al. 2010; Gilbert et al. 2011) and glycolipids (Vincent and Klig 1995; Heise et al. 2002; Rittershaus et al. 2006; Castle et al. 2008). These compounds are essential for maintaining cellular homeostasis and establishing infection. Synthesis of many glycoconjugates relies on activated donor molecules, such as nucleotide sugars, from which individual sugar moieties are transferred to a growing glycan structure. Nucleotide sugars are generally made in the cytosol and then transported into the secretory organelles (endoplasmic reticulum and/or Golgi apparatus) where most glycan biosynthesis occurs (Varki et al. 2009). Nucleotide sugar transporters (NSTs) mediate transport of these highly charged compounds by importing them in exchange for the corresponding nucleotide monophosphates via an antiport mechanism (Abeijon et al. 1997; Berninsone and Hirschberg 2000). This makes the nucleotide sugars available for use by the luminal glycosyltransferase enzymes that synthesize capsule polymers or other glycans.

The capsule polysaccharides are composed of galactose (Gal), Gal_f, GlcA, Man and Xyl; this suggests that their synthesis requires the corresponding donors, which are UDP-Gal, UDP-Gal_f, UDP-GlcA, GDP-Man and UDP-Xyl. The enzymatic pathways required for synthesis of these compounds in *C. neoformans* have been elucidated (Bar-Peled et al. 2001; Wills et al. 2001; Bar-Peled et al. 2004; Griffith et al. 2004; Beverley et al. 2005; Moyrand et al. 2008), but the identity and the regulation of most of the NSTs that translocate them into the secretory pathway remain elusive. Only transport of the mannose donor, GDP-mannose, has been demonstrated biochemically (Cottrell et al. 2007).

Strains deficient in UDP-Gal synthesis have aberrant capsule, likely due to perturbed GXMGal production, and are completely avirulent, emphasizing the critical role of this nucleotide sugar (Moyrand et al. 2008). A UDP-Gal transporter, Ugt1, was initially identified by homology to known UDP-Gal transporters (Moyrand et al. 2007), which are found ubiquitously in eukaryotes. However, sequence identity does not tell the whole story of NST substrate specificity (Martinez-Duncker et al. 2003). For example, cells may express several NSTs with overlapping specificities but non-identical substrate affinities. Some transporters are highly selective for a specific substrate, while others transport as many as four distinct nucleotide sugars (Berninsone et al. 2001; Norambuena et al. 2002; Segawa et al. 2002; Aoki et al. 2003; Ashikov et al. 2005; Segawa et al. 2005; Caffaro et al. 2008). Finally, transport activity may also be influenced by association with glycan synthetic enzymes and by subcellular localization (Maszczak-Seneczko et al. 2012). Although the absence of galactose in total capsular polysaccharide and whole cell preparations from *ugt1*Δ mutants (Moyrand et al. 2007) provides indirect evidence that UDP-galactose is a Ugt1 substrate, defining NST activity requires biochemical demonstration of function.

Here we directly interrogated the biochemical activity of Ugt1, motivated by the central role of galactose in cryptococcal virulence and the gaps in our knowledge of *C. neoformans* NSTs (Moyrand et al. 2007). We found that Ugt1 transports both UDP-Gal and UDP-*N*-acetylgalactosamine (GalNAc) in vitro and that this function does not depend on the extended cytosolic termini of the protein. Furthermore, cells lacking Ugt1 exhibit growth and mating defects, along with altered capsule and cellular morphology. Finally, the mutant was phagocytosed more readily by macrophages and cleared more quickly in vivo and in vitro. Our studies define the biochemical role of this important protein, and suggest mechanisms for the reduced virulence of cells lacking this transporter.

Materials and methods

Sequence and phylogenetic analysis

UGT1 was identified by BLASTP searches against *C. neoformans* predicted proteins (Broad Institute; *C. neoformans* var. grubii H99 database) using known UDP-galactose transporters from *Schizosaccharomyces pombe* (NP_588041), *Arabidopsis thaliana* (NP_565158.1), *Caenorhabditis elegans* (NP_001255676.1) and *Homo sapiens* (NC_000023.11). Alignments were performed using the ClustalW program at Jalview 2.0 Alignment Annotator (http://www.bioinformatics.org/strap/aa/) with default settings (Waterhouse et al. 2009). Transmembrane domains of Ugt1 were predicted using TMHMM server v 2.0 (Center for Biological Sequence Analysis, Technical University of Denmark). Protter (http://wlab.ethz.ch/protter/start/) was used to visualize putative protein topology. Multiple sequence alignment (MUSCLE; Edgar 2004), phylogenetic analysis (PhyML; Guindon and Gascuel 2003) and tree rendering (TreeDyn; Chevenet et al. 2006) of Ugt1 and characterized human NSTs was done using the online Phylogeny.fr program (http://www.phylogeny.fr/version2_cgi/index.cgi) with default settings (Dereeper et al. 2008; Dereeper et al. 2010).

Cell growth

Unless otherwise noted, *C. neoformans* strains (Table I) were grown at 30°C in YPD medium (1% [wt/vol] Bacto Yeast Extract, 2% [wt/vol] BactoPeptone and 2% [wt/vol] dextrose) with shaking (230 rpm). For phenotypic analysis, cells from overnight (O/N) cultures were washed in sterile phosphate-buffered saline (PBS), resuspended at 10^7 cells/mL in PBS, and 5 µl aliquots of 5 or 10-fold serial dilutions were plated and grown at 30 or 37°C as indicated. Conditions tested included YPD containing 0.005% sodium dodecyl sulfate (SDS), 2 M sorbitol, 10 mM H_2O_2 or 0.05% Congo Red. Mating was assayed at 25°C on 5% V8 juice agar medium, pH = 5.25 (Kwon-Chung et al. 1992).

C. neoformans strains and plasmids

We used a split marker strategy (Fu et al. 2006) to replace *UGT1* with a nourseothricin (NAT) resistance marker, selecting

Table I. *C. neoformans* strains used in these studies

C. neoformans strain[a]	Serotype	Origin
KN433	D	Nielsen et al. (2005)
KN433 *ugt1*	D	This study
KN433 *ugt1::UGT1*	D	This study
Jec21	D	Kwon-Chung et al. (1992)
Jec21 *CXT1*-myc	D	Reilly et al. (2011)
Jec21 *CXT1*-myc *UGT1*-HA	D	This study
Jec21 *CXT1*-myc *GMT1*-HA	D	Wang et al. (2014)
KN99**a**	A	Nielsen et al. (2003)

[a]All strains are MATα except for KN99**a**.

Table II. Primers used for modification of or expression in *C. neoformans*

Primer	Sequence (5′–3′)
1	CCGGCGCGCCGTTTAAACTCATGCGTAATCCGG AACGTCGTAGGGGTAACCATGCTTTCTATCAA TGTCCAAAC
2	CCCTAGCTAGCGTTTAAACATGGCCCATCGAACC AACACTCG
3	GTCACGAAGAATTCGTGGGCTATGCTACTGCGATG
4	TACCTCGGCGCGGCCGCTTAACCATGCTTTCTATC
5	GTCACGAAGAATTCGCCCATCGAACCAACACT
6	GTCACGAACCTAGGCTAGATTGGCGGAGCGGGGCT
7	GTCACGAACCTAGGTCAACCATGCTTTCTATCAATG
8	GTCACGAACACGTGATGGACTACAAGGACGATGACG
9	GTCACGAACCTAGGGATTGGCGAGCGGGGCT
10	GAATTCGCCCATCGAACCAACAT
11	CTCGAGTTAACCATGCTTTCTATC

transformants on NAT-containing plates for PCR verification of gene replacement. We used a similar strategy to complement the *ugt1* deletion strain at the endogenous locus, by replacing the NAT deletion cassette with *UGT1* in tandem with a geneticin (G418) resistance marker. Transformants of interest were identified by resistance to G418 and sensitivity to NAT, consistent with replacement of the deletion cassette by *UGT1* in tandem with the G418 marker. All complemented strains were verified by PCR (data not shown) and reversal of phenotypes (see *Results*).

For protein localization, a construct encoding C-terminally HA-tagged Ugt1 (pUGT1-HA) was generated by amplification of *UGT1* from genomic Jec21 DNA with Primers 1–2 (Table II) to incorporate sequence encoding the tag, subcloning into pCR2.1 (LifeTechnologies; Carlsbad, CA) for sequencing, and then PmeI digestion with ligation to pMSC043 to incorporate a NAT resistance marker and place the tagged protein under the actin promoter. pUGT1-HA was linearized with I-sceI and transformed into the Cxt1-myc strain (Reilly et al. 2011) by biolistic transformation. Transformants were selected by growth on NAT plates and verified by immunoblotting.

To episomally complement *ugt1*Δ, N- and C-terminally truncated and full-length Ugt1 constructs were generated from Jec21 cDNA by amplification with Primers 3–4, 5–6, and 7–8, respectively (Table II). The DNA fragments were then digested with EcoRI/NotI and subcloned into pYEScupFLAG*K* (Ashikov et al. 2005) to add an N-terminal FLAG-tag and facilitate sequencing. The resulting FLAG-tagged constructs were amplified with Primers 9–10 or 10–11 (Table II), and digested with PmlI/AvrII for ligation into pMSC042-neo to incorporate a G418 resistance marker and place *UGT1* under control of the actin promoter. The plasmids were subsequently linearized with I-SceI and electroporated into *ugt1*Δ. Transformants were selected by growth on G418 plates and verified by PCR.

Localization

JEC21 *CXT1-myc* (Cottrell et al. 2007) alone or expressing Ugt1-HA or Gmt1-HA was prepared for microscopy as described by Reilly et al. (2011) with minor modifications. Briefly, cells were grown O/N in YPD before fixation and blocking, and slides were then incubated with high-affinity rat anti-hemagglutinin (anti-HA) monoclonal antibody (Roche Applied Science; Denzberg, Germany; 20 ng/mL in blocking buffer), mouse anti-c-Myc (anti-myc) antibody (Abcam; Cambridge, UK; 5 μg/mL in blocking buffer) or blocking buffer alone. This was followed by incubation with the appropriate secondary antibody, either Alexa Fluor 594-tagged goat anti-rat IgG or Alexa Fluor 488-tagged goat anti-mouse IgG (Invitrogen; Carlsbad, CA), at 1 μg/mL in blocking buffer.

For localization studies in MDCKII cells, human SLC35A2 (BAA95615) or cryptococcal *UGT1* (EAL18940) were amplified so as to encode a C-terminal HA-tag, cloned into the PmeI site of pcDNA3.1 (LifeTechnologies) to form phUGT1-HA or pcUGT1-HA, respectively, and verified by sequencing. MDCKII cells seeded to 5×10^4 cells/cm^2 in a 6-well plate were then transiently transfected with 1 μg of pcDNA3.1, pcUGT1-HA or phUGT1-HA. For transfection, the DNA and lipofectamine (LifeTechnologies) were incubated at room temperature (RT) for 15 min and added to cells for incubation at 37°C/5% CO_2 for 3 h. Cells were then washed and incubated in minimal essential media (MEM; LifeTechnologies) + 10% FCS O/N before being plated on cover slips in a 12-well plate. After 24 h at 37°C/5% CO_2, the cover slips were fixed in 4% formaldehyde/PBS for 20 min, and the cells were permeabilized with 5% BSA in 0.3% TX-100 in PBS for 15 min and stained with rabbit anti-Giantin IgG (Abcam; 200 ng/mL in blocking buffer) and rat anti-HA (Invitrogen; 20 ng/mL in blocking buffer). Finally, cells were incubated for 20 min with AlexaFluor 594-tagged goat anti-rat IgG and AlexaFluor 488-tagged goat anti-rabbit IgG (Invitrogen; 1 μg/mL in blocking buffer) and viewed with a ZEISS Axioskop2 MOT Plus microscope using a 63 × objective. Where not specified, all steps were performed at RT.

Lec cell complementation

Lec8 cells were transiently transfected with pcDNA3.1, pcUGT1-HA or phUGT1-HA as described for the MDCKII studies. Cover slips were then fixed with 3.7% formaldehyde for 30 min, washed twice with PBS, and permeabilized with 0.1% TX-100/PBS for 30 min. After blocking in 1% BSA/PBS for 10 min, cells were stained with fluorescein isothiocyanate (FITC)-conjugated GSII in blocking buffer for 30 min at 37°C, rat anti-HA for 1 h and AlexaFluor 594-tagged goat anti-rat IgG for 1 h. Samples were viewed with a ZEISS Axioskop2 MOT Plus microscope using a 63 × objective. Where not specified, steps were performed at RT.

Ugt1 truncations (Table III) were assessed in a Lec8 cell line stably transformed with the polyomavirus large T antigen (CHOP8) as described by (Bakker et al. 2005). Briefly, CHOP8 cells were transfected with the vector pEFBO encoding the rat β-1,3-glucuronyltransferase (Terayama et al. 1997), and plasmids expressing each Ugt1 variant were generated using the primers in Table IV. After 3 days at 37°C/5% CO_2, cells were fixed, blocked in 2% milk/TBS and then stained with rat monoclonal L2-412 (Kruse et al. 1984; Bakker et al. 1997) followed by goat anti-rat alkaline phosphatase

Table III. Ugt1 truncations and their ability to complement UDP-Gal transport

UGT1 variant	Amino acids	CHOP8 complementation
Full length	1–703	+
N1	56–703	+
N2	76–703	+
N3	109–703	+
N4	168–703	+
N5	212–703	–
N6	254–703	–
C1	1–571	+
N6/C1	254–571	–

Table IV. Primers used to generate truncation constructs for Lec8 expression

UGT1 variant	Primer sequence
Full length	5′-ATCGAATTCGCCCATCGAACCAACACT-3′ 5′-TTAACCATGCTTTCTATC-3′
N1	5′-ACTAGAATTCAGAGATCGAAGCGAGAGA-3′ 5′-TTAACCATGCTTTCTATC-3′
N2	5′-ACTAGAATTCGGGAAGACGCGCGGTATGGA-3′ 5′-TTAACCATGCTTTCTATC-3′
N3	5′-ACTAGAATTCTCCTCTACCTCTGTCAGCT-3′ 5′-TTAACCATGCTTTCTATC-3′
N4	5′-ACTAGAATTCGTGGGCTATGCTACTGCGA-3′ 5′-TTAACCATGCTTTCTATC-3′
N5	5′-ACTAGAATTCCACTATTCACGGATATCTA-3′ 5′-TTAACCATGCTTTCTATC-3′
N6	5′-ACTAGAATTCACTGCATCTCCTCCTC-3′ 5′-TTAACCATGCTTTCTATC-3′
C1	5′-ATCGAATTCGCCCATCGAACCAACACT-3′ 5′-ACACTCGAGACTGGCAGGTGGAGCGGGGCT-3′

in blocking solution. Samples were then treated with Fast-Red substrate (Sigma-Aldrich; St. Louis, MO) to allow enumeration of red cells per plate by light microscopy.

S. cerevisiae expression and transport assays

Yeast expression experiments were done in *S. cerevisiae* strain YPH500 (*MATα ura3-52 lys2-801 ade2-101 trp1-Δ 63 his3-Δ200 leu2-Δ1*). *UGT1* was amplified from JEC21 RNA using Primers 10 and 11, cloned into pCR2.1 (TOPO TA, LifeTechnologies) and sequenced. The fragment was then digested with EcoRI and XbaI, ligated into the copper-inducible expression vector pYEScupFLAG*K* (Ashikov et al. 2005) and transformed into YPH500 cells using lithium acetate (Invitrogen).

S. cerevisiae cells transformed with empty pYEScupFLAG*K* or pYEScupFLAG*K*-UGT1 were grown in 0.5 mM $CuSO_4$-supplemented selective medium (0.67% Bacto-yeast nitrogen base without amino acids, L-leucine, L-histidine, L-tryptophan, L-lysine, adenine, 2% glucose) for 2 h to induce protein expression. Golgi membranes were isolated by subcellular fractionation and then assayed for the ability to import radiolabeled nucleotide sugars (NEM Life Science Products; Boston, MA) as described by Ashikov et al. (2005). Transport of each assay substrate by strains with empty or Ugt1-expressing vectors was compared by unpaired Student's *t*-test.

Capsule induction

O/N cultures of *C. neoformans* grown in YPD were collected by centrifugation and washed twice with sterile PBS. Cells were then either resuspended in Dulbecco's Modified Eagle's Medium (DMEM; Sigma-Aldrich) at 10^6 cells/mL in T-75 tissue culture flasks and incubated at 37°C in 5% CO_2 for 24 h or diluted to 5×10^6 cells/mL in 10% Sabouraud's medium (4% [wt/vol] dextrose, 2% [wt/vol] peptone, pH = 5.6) in PBS and grown at 30°C with shaking for 48 h. Cells were collected, washed twice in PBS, resuspended in PBS, mixed with 1.5 parts India ink and viewed with a ZEISS Axioskop2 MOT Plus microscope, 63 × objective.

Fungal gene expression

Wild-type (WT) cells cultured in YPD were grown in DMEM under capsule-inducing conditions and sampled at 0, 1.5, 3, 8 and 24 h for ribonucleic acid (RNA) isolation and sequencing. See Maier et al. (2015) for details.

Transmission electron microscopy

Strains were grown in Sabouraud's capsule-inducing conditions (Zaragoza and Casadevall 2004), collected by centrifugation (3000 × *g*; 5 min), fixed for 1 h at RT with 2% glutaraldehyde (Polysciences Inc.; Warrington, PA) in 100 mM phosphate buffer (pH 7.2) and then incubated for 1 h in 1% osmium tetroxide (Polysciences Inc.). Following dehydration with ethanol and propylene oxide, cells were embedded in Eponate 12 resin (Tel Pella Inc.; Redding, CA), and 70–90 nm sections were cut with an UCT ultramicrotome (Leica Microsystems Inc.; Buffalo Grove, IL). Sections were stained with uranyl acetate and lead citrate for visualization with a JEOL 1200EX transmission electron microscope (Jeol Inc.; Peabody, MA).

Macrophage assays

To assay fungal survival in macrophages, THP-1 monocytes were seeded at 3.5×10^5 cells/well in a 96-well plate, treated with 0.2 ug/mL PMA for 72 h to induce differentiation and incubated with *C. neoformans* at MOI = 0.1 for 1 h at 37°C and 5% CO_2. Plates were washed twice with PBS, and samples incubated for 1 or 24 h before lysis and plating in triplicate on YPD agar for counts of colony-forming units (CFU).

Macrophage phagocytosis of fungal strains was quantified using our previously published assay (Srikanta et al. 2011) with minor modifications. Briefly, cells were grown in capsule-inducing media as above or in parallel YPD cultures. Cells were then collected by centrifugation, washed and opsonized with commercial human serum before incubation with differentiated THP-1 macrophages for 1 h. Host cell cytosol and nuclei and fungal walls were stained, and samples were imaged on a Cytation3 plate reader (BioTek; Winooski, VT) and analyzed using IN Cell Developer Toolbox 1.9.2 (GE Healthcare Life Sciences; Pittsburgh, PA). Assay results for *ugt1Δ* were compared to those for WT and complemented strains by analysis of variance (ANOVA).

Animal studies

Fungal strains to be tested were cultured O/N in YPD, washed in PBS and diluted to 2.5×10^4 cells/mL in sterile PBS. The 50 µl aliquots were then inoculated intranasally into six 4- to 6-week-old female C57Bl/6 mice (NCI, National Institutes of Health). Groups of two and four mice were sacrificed at 1 h and 7 days

postinoculation, respectively. Initial inocula and lung homogenates were plated for CFU, and organ burden was analyzed by ANOVA. All studies were performed in compliance with institutional guidelines for animal experimentation.

Results

C. neoformans strains are classified into four serotypes: A and D are associated with cryptococcosis in immunocompromised populations, while B and C are associated with disease in otherwise healthy individuals. We initially identified *UGT1* in serotype A, which is the most prevalent serotype and causes most of the mortality from this disease (Kwon-Chung and Varma 2006), and subsequently identified homologs with 92–95% identity at the protein level in the other serotypes (protein accession numbers: XP_012048733, KIR46271, KIR59644 and XP_568024 for serotypes A through D, respectively). Phylogenetic analysis of the serotype D *UGT1* sequence together with characterized human NSTs places Ugt1 in the SLC35A subfamily, along with its human counterpart (Figure 1). Similar to other transporters, it is predicted to have an even number of transmembrane domains (here 10) with cytosolic N- and C-termini (Figure 2). The predicted cytosolic termini are unique and unusually long (Figure 2), at least five times longer than those of other known UDP-Gal transporters with no significant sequence similarity (not shown). The NST domain of Ugt1 (aa 299–558) also shares less than 50% identity to those proteins (Supplementary data, Figure S1).

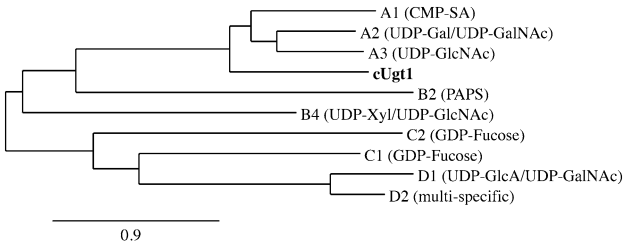

Fig. 1. Phylogenetic relationships of cryptococcal Ugt1 (bold) and human NSTs with known substrates (in parentheses). Tree reconstruction was performed with the Phylogeny.fr web server (Dereeper et al. 2008, 2010) using MUSCLE, PhyML and TreeDyn software. Human transporters are denoted by their SLC35 family designation, and distance is expressed as the number of amino acid substitutions per 100 positions.

We next investigated Ugt1 localization by comparing staining of episomally expressed Ugt1-HA to that of a known Golgi xylosyltransferase, Cxt1p, which we have tagged with myc (Reilly et al. 2011). When we probed doubly tagged cryptococci with both anti-HA and anti-myc antibodies, we observed co-staining of large perinuclear puncta, suggesting Golgi localization of Ugt1 (Supplementary data, Figure S2). This localization is consistent with a role for this protein in providing raw materials for glycan synthesis to processes occurring in the secretory pathway. Because the inherent challenges of immunostaining this yeast limit image quality, we also localized HA-tagged human and cryptococcal Ugt1 in MDCKII cells. In this higher resolution analysis, both proteins colocalized with the Golgi marker giantin (Figure 3A), supporting our *C. neoformans* results.

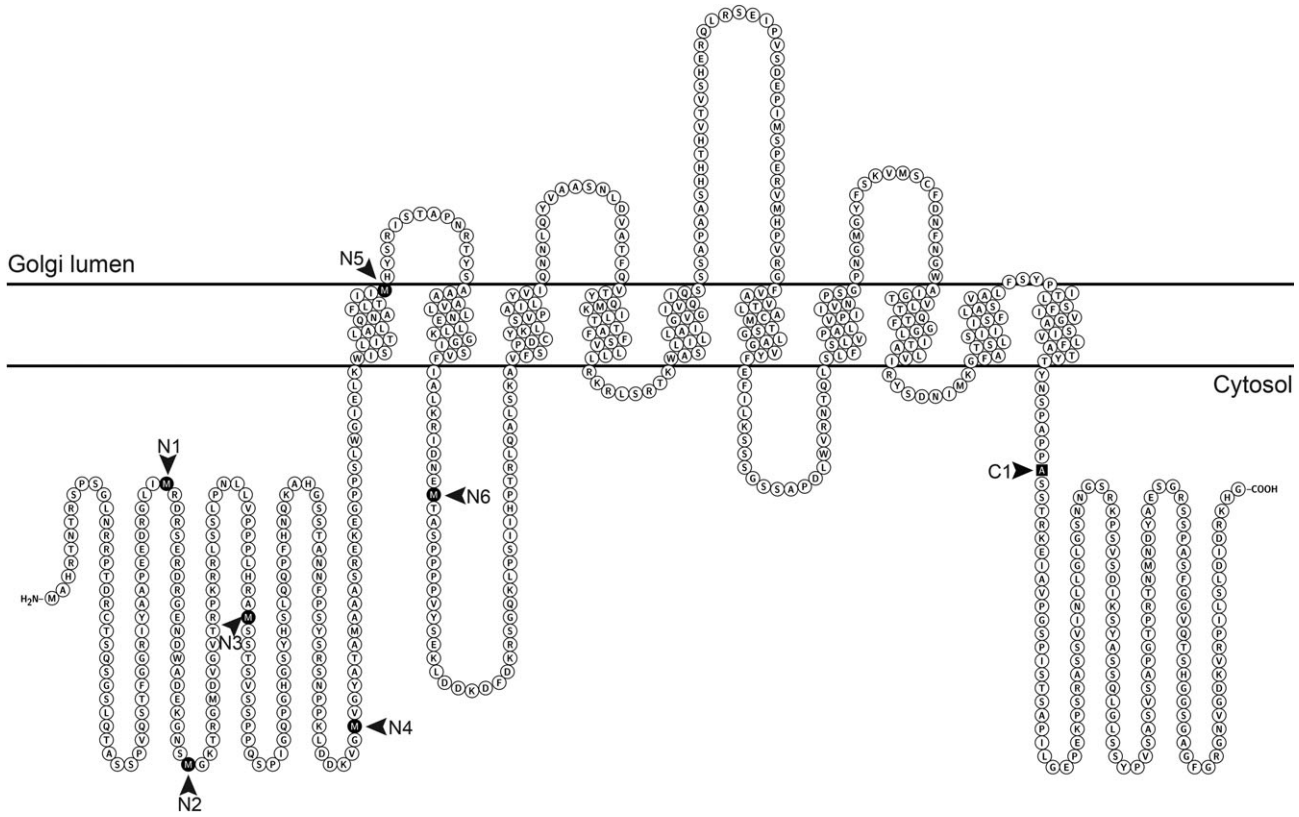

Fig. 2. Topology of *C. neoformans* Ugt1 as predicted by TMHMM server v 2.0, showing 10 putative transmembrane domains and long N- and C-terminal cytosolic tails. Arrowheads indicate the new N-terminus for each N-terminal truncation and the terminal residue of the single C-terminal truncation (C1); see text and Table III for details.

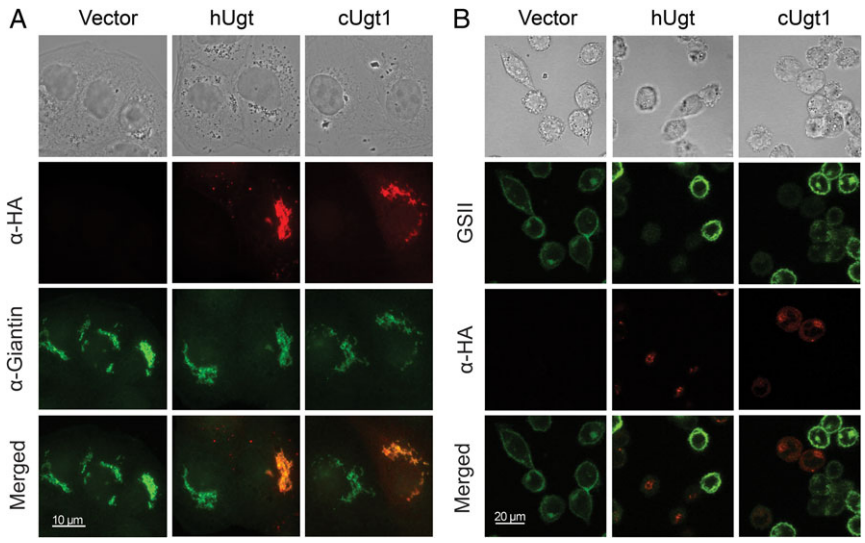

Fig. 3. The cryptococcal UDP-Gal transporter localizes with a Golgi marker and is functional in mammalian cells. (**A**) MDCKII cells transiently transfected with vector alone (vector) or vector expressing HA-tagged forms of the human UDP-Gal transporter (hUgt) or cryptococcal UDP-Gal transporter (cUgt1) were probed with antibodies to HA and to the Golgi protein giantin (as indicated above). As expected, all cells stain with the Golgi marker, while a subset expresses each colocalizing transporter. (**B**) Lec8 cells were transiently transfected with the same constructs as in Panel A and probed with anti-HA antibody and GSII-FITC (a lectin specific for terminal GlcNac) (denoted above). Terminal galactose modification of cell surface glycans, which prevents the lectin binding, occurs only in cells that express a UDP-Gal transporter. Bright field and merged images are shown (Panel A scale bar, 10 μm; Panel B scale bar, 20 μm). α-HA, red; α-Giantin and GSII, green. This figure is available in black and white in print and in color at *Glycobiology* online.

The mammalian Lec8 cell line is deficient in UDP-Gal transport (Deutscher and Hirschberg 1986; Oelmann et al. 2001). We used transient transfection to assess whether the cryptococcal transporter could complement this defect, using *Griffonia simplicifolia* lectin (GSII) as a reporter. This lectin binds terminal GlcNAc residues, which are masked in normal cells by galactose added in the secretory pathway. In cells lacking UDP-Gal transport, this galactose modification is absent, so the lectin is able to bind to the cell surfaces. Expression of cryptococcal Ugt1 reversed this binding (Figure 3B). Notably, the subset of transiently transfected cells that did not express exogenous protein still bound the lectin (Figure 3B), serving as an internal control. This staining pattern was mirrored by expression of the human UDP-Gal transporter, strongly supporting shared biochemical activity of the two proteins.

To directly measure the activity of the cryptococcal transporter, we used heterologous expression in *S. cerevisiae*. When we assessed the transport of a panel of radiolabeled nucleotide sugars in vitro, Golgi vesicles from cells expressing cryptococcal Ugt1 demonstrated transport of UDP-Gal, as predicted by homology, as well as somewhat lower transport of UDP-GalNAc (Figure 4). We did not detect transport over background of other capsule precursors (UDP-Xyl or UDP-GlcA), UDP-GlcNAc or UDP-Glc.

We had noted the unusual length of the N- and C-terminal cytosolic tails of Ugt1, and wondered whether they were required for its transport activity. To test this, we used transient transfection to determine which of a series of Ugt1 truncation variants (Figure 2) could complement the deficient UDP-Gal transport of CHOP8 cells, which are derived from Lec8 cells (see *Methods*). We detected activity by cotransfection with DNA encoding a rat β-1,3-glucuronyltransferase, such that the combination could support the synthesis of GlcUAβ1,3Gal epitopes; these are recognized by the antibody L2-412 (Kruse et al. 1984; Bakker et al. 1997). As shown in Table III, all the cytosolic tail truncations that we tested (Figure 2) retained activity; function was only disrupted when the truncation was extended beyond the first transmembrane domain.

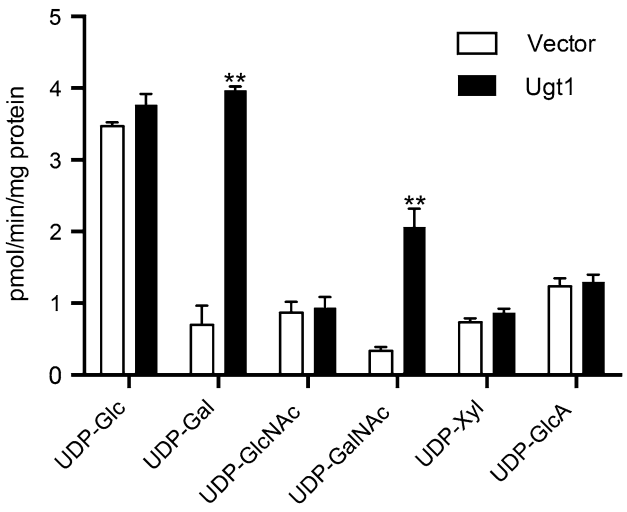

Fig. 4. Ugt1 transports UDP-Gal and UDP-GalNAc. Golgi fractions isolated from *S. cerevisiae* expressing vector alone (white bars) or *UGT1* (black bars) were assayed for transport of the indicated nucleotide sugars. Each value represents the mean and the standard deviation of duplicate assays from three independent Golgi preps. **, $P < 0.001$ compared with vector alone.

Because galactose is a major component of one capsule polysaccharide, GXMGal, we examined the expression of *UGT1* and other genes related to galactose metabolism under growth conditions that induce capsule synthesis. RNA-seq analysis indicated that both *UGT1* and *UGE1*, a gene encoding a UDP-glucose epimerase (which catalyzes the interconversion of UDP-glucose and UDP-Gal), are upregulated several fold under these conditions (Figure 5), consistent with a role for both proteins in capsule synthesis. A *UGE1* paralog, *UGE2*, remains at basal levels during capsule induction (Figure 5); the corresponding mutant also has no defects in capsule synthesis or virulence (Moyrand et al. 2008). Other genes involved

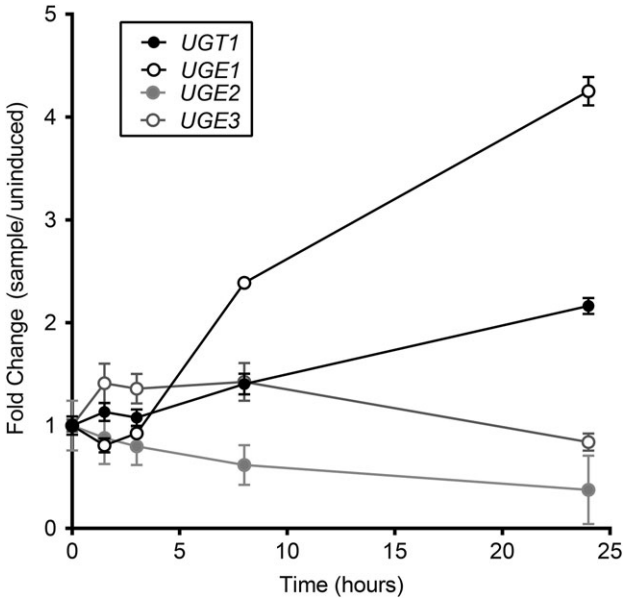

Fig. 5. Transcription of *UGT1* and *UGE1* increases during capsule induction. Reads from RNA-seq data (mean ± SD) were normalized to their levels at $t = 0$, which were *UGT1*, 383,949 ± 24,018; *UGE1*, 724,792 ± 19,475; *UGE2*, 110,719 ± 18,909; *UGE3*, 1968117 ± 82297. Values shown are compiled from three independent experiments, each with RNA prepared from three biological replicates.

in UDP-Gal metabolism (galactokinase and galactose-1-phosphate uridylyltransferase) showed no change or less 2-fold reduction in expression over the same time course of induction (data not shown).

We next directly examined the effect of deleting *UGT1* on capsule morphology. When we grew cells in noncapsule-inducing conditions (the rich yeast medium YPD), both WT and mutant cells had thin capsules, which were minimally discernible by negative staining (Figure 6A, first column). Capsules of both strains were also similarly enlarged when the cells were grown in our standard capsule-inducing conditions (DMEM at 37°C and 5% CO_2; Figure 6A, second column), which were also used for the expression profiling above. Because serotype A cells lacking *UGT1* had previously been reported to be hypercapsular (Moyrand et al. 2007), which we did not observe in the DMEM conditions, we tested other inducing media. We found that *ugt1*Δ cells grown in 10% Sabouraud's media were hypercapsular compared to WT cells (Figure 6A, third column). The capsule fibers of mutant cells grown in this medium were also markedly longer by electron microscopy (Figure 6A fourth column); these phenotypes were reversed by complementation of the mutant. In all conditions, the mutant cells tended to aggregate, which suggested altered surface properties independent of capsule formation.

Cryptococcal glycans have not been exhaustively analyzed, but galactose is a known component of cryptococcal glycolipids (Wohlschlager et al. 2013) and capsule polysaccharides, and may occur in other glycoconjugates as well. For this reason, we tested

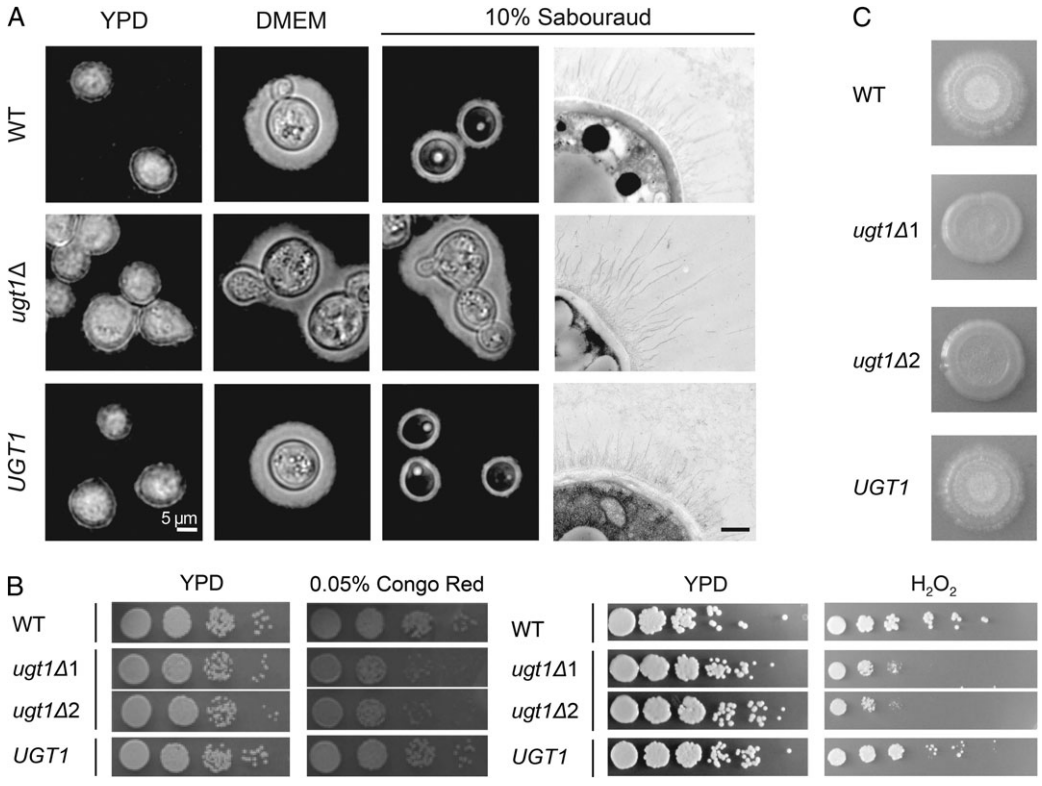

Fig. 6. *ugt1*Δ mutants show altered capsule and cellular morphology, and exhibit growth and mating defects. (**A**) Wild-type (WT), *ugt1*Δ and complemented *ugt1*Δ (*UGT1*) were grown in the media noted above and visualized by light microscopy after negative staining with India Ink (first three columns, scale bar = 5 μm) or by electron microscopy (last column, scale bar = 500 nm). (**B**) The indicated strains, including two independent *ugt1*Δ strains, were grown overnight at 30°C in YPD, and 5 μl of serial dilutions were spotted and grown as indicated. Left panel, dilutions were 10-fold starting at 10^6 cells; right panel, dilutions were 5-fold, starting at 10^7 cells. (**C**) Equal volumes of the indicated MATα strains and KN99**a** were mixed, spotted on V8 agar and incubated at RT in the dark. Images were taken 2 weeks after initial spotting. In three independent experiments, no filamentation of either mutant strain was detected.

other characteristics of cells lacking Ugt1. We noted that *ugt1*Δ cells were significantly more sensitive than WT to Congo Red dye, suggesting a cell wall defect (Figure 6B). This strain was also sensitive to H_2O_2 (Figure 6B), in addition to high temperature and SDS (properties previously reported for the corresponding serotype A mutant (Moyrand et al. 2007), which we verified for serotype D (not shown)). The mutant cells were also defective in mating, failing to form filaments and spores when cocultured on solid media with cells of the opposite mating type (Figure 6C). In all cases, the WT phenotypes were restored in the complemented mutant.

We wondered whether the extended termini of Ugt1, which were not required for transport activity (Table III), might influence cell phenotypes. To test this, we episomally complemented *ugt1*Δ with WT *UGT1*, or *UGT1* modified, so its product lacked either the N- or C-terminus, all under control of the constitutive actin promoter. All three construct-expressing strains restored WT resistance to stress but also exhibited larger capsules than WT cells. Interestingly, the full-length and C-terminally truncated *UGT1* produced considerably larger capsules than WT cells (1.8- and 1.6-fold greater than WT, respectively; Figure 7A). They also demonstrated greater growth on NaCl but not on any of the other conditions tested (Figure 7B) (see *Discussion*).

The observed changes in surface properties and reduced ability to resist stress of the mutant strongly suggested that its interactions with host cells would be aberrant. To test this, we first used an automated high-throughput imaging method (Srikanta et al. 2011) to quantify the early interactions between a human monocytic cell line (THP-1) and each strain. As in the previous work, unopsonized fungi were poorly phagocytosed. For opsonized samples, we found that when the yeast had been cultured in rich medium (YPD or Sabouraud's broth), *ugt1*Δ was engulfed at significantly higher rates than WT (Figure 8A). This was independent of capsule size, as WT and mutant cells both produce minimal capsule in YPD (Figure 6A). In contrast, after culturing in conditions where WT and mutant displayed equally large capsules (Figure 6A, DMEM), phagocytosis of all strains was similar (Figure 8A). We also tested the relative survival of internalized fungi during a 24-h period. We found that the mutant cell population increased more slowly than WT or complemented strains within host phagocytes, reflecting poor growth and/or increased destruction by the host cells (Figure 8B).

The combination of defects we observed in *ugt1*Δ suggested that this strain would do poorly in an infected host, as previously observed in a model based on tail vein infection (Moyrand et al. 2007). We tested this in mice infected intranasally, which mimics the natural route of infection. In this model, *ugt1*Δ was completely cleared from the lungs by 7 days after inoculation, in contrast to WT and complement infected mice (average $\log_{10}$CFU/mL at 7dpi: WT, 2.76; *ugt1*Δ, 0; *UGT1*, 2.33). This rapid clearance of the mutant supports the key role of Ugt1 in cryptococcal biology.

Discussion

C. neoformans encodes a single functional UDP-Gal/UDP-GalNAc transporter, which is homologous to UGTs found across multiple

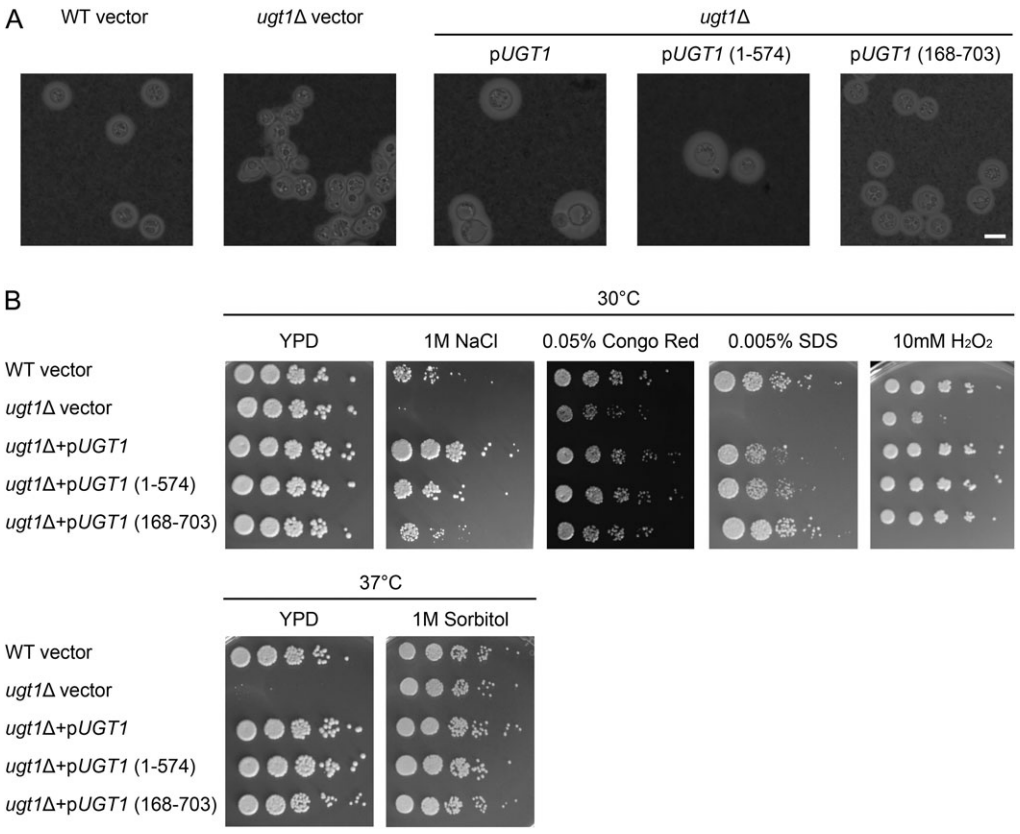

Fig. 7. N- and C-terminal UGT1 truncations complement capsule and cellular morphology defects in *ugt1*Δ. (**A**) The strains indicated above the horizontal line, carrying the plasmids shown below the line, were grown in DMEM + G418 and visualized by light microscopy after negative staining with India Ink (scale bar = 5 μm). (**B**) The indicated strain and plasmid combinations were grown overnight at 30°C in YPD + G418. The 5 μl of serial dilutions were spotted and grown as indicated with G418 (except for 0.005% SDS). Dilutions were 5-fold starting at 10^6 cells.

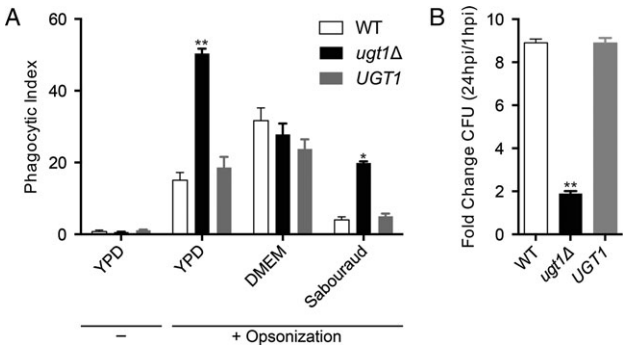

Fig. 8. Cells lacking Ugt1 are more efficiently phagocytosed and killed by THP-1 cells than wild-type *C. neoformans*. (**A**) Phagocytic index (engulfed fungi/100 host cells) of strains grown in YPD (–/+ opsonization) or in inducing media (+ opsonization). (**B**) Survival of YPD-grown, opsonized fungi after internalization by THP-1 cells. Data are representative of three independent experiments performed with $n = 3$ (*, $P < 0.01$; **, $P < 0.001$).

phyla (e.g. *H. sapiens*, *C. elegans*, *S. pombe*, *A. thaliana*; Supplementary data Figure S1). This protein is predicted to have 10 transmembrane segments with N- and C-terminal tails in the cytosol (Figure 2) and is localized to the Golgi apparatus (Figure 3A, Supplementary data Figure S2), consistent with other transporters in this family. Alignment of Ugt1 and known transporters, however, did not reveal any common motif that would potentially confer UDP-Gal or UDP-GalNAc specificity (Supplementary data Figure S1).

We demonstrated that cryptococcal Ugt1 transports UDP-Gal both indirectly, through complementation of Lec8 cells (Figure 3B), and directly, by performing transport assays in a heterologous system (Figure 4). Of the other potential substrates tested (Figure 4), we only observed transport of UDP-GalNAc. Human and *Drosophila* UGTs similarly recognize this combination of substrates, although only the human and cryptococcal UGTs transport UDP-Gal more efficiently than UDP-GalNAc (Figure 4; Segawa et al. 2002). Galactose is an abundant component of cryptococcal capsule and is also known to be incorporated into some of its glycolipids. GalNAc, in contrast, has not been detected in any cryptococcal glycans to date, but this does not preclude the possibility that small amounts are incorporated into these structures, particularly as the synthetic machinery for UDP-GalNAc is encoded in the cryptococcal genome.

Specific recognition of multiple substrates with the same nucleotide portion is common among NSTs, with the nucleotide-binding specificity mediated by the cytosolic domains (Abeijon et al. 1997). The cryptococcal Ugt1 is noteworthy for having unusually long cytosolic tails, which stimulated us to pursue their function. The first transmembrane helix of human SLC35A2 is required for UDP-Gal transport (Aoki et al. 2001); we similarly found that the first transmembrane domain of the cryptococcal protein was needed for transport in mammalian cells, although both cytosolic tails were dispensable (Figure 2 and Table III). In *C. neoformans*, episomal expression of *Ugt1* truncations that spared the transmembrane domains also restored WT capsule and stress resistance to *ugt1*Δ (Figure 7), supporting the dispensability of the cytosolic domains for transport activity. Notably, constitutive episomal expression of full-length Ugt1 (or the C-terminal truncation) yielded capsules that were larger than those of WT cells (Figure 7A), and appeared to confer an increased salt tolerance (Figure 7B). One potential explanation of these findings is that Ugt1 overexpression impacts the quantity or composition and structure of cellular glycoconjugates, perhaps through greater incorporation of galactose, producing larger capsules and modulating stress resistance pathways. The inability of N-terminal mutants to produce capsules as large as mutants expressing full-length and C-terminal Ugt1 thus suggests that, while the N-terminus is not absolutely required for substrate recognition and transport, it may modulate the efficiency of those processes or additional downstream glycosylation reaction(s). The N-terminus of Ugt1 might impact these processes by mediating interactions with capsule-associated glycosyltransferases, influencing oligomerization-based regulation, or regulating binding of regulatory proteins (Hadley et al. 2014). It will be of interest in the future to further elucidate the role of these domains.

When we examined the transcriptional profile of *C. neoformans* under conditions that induce capsule production, and thus presumably UDP-Gal utilization, we observed that *UGT1* and *UGE1* expression are significantly upregulated within 8 h (Figure 5). Other genes implicated in galactose metabolism demonstrated less than a 2-fold change in either direction, perhaps not surprising since strains were grown with glucose as the primary carbon source. *C. neoformans* thus seems to satisfy the greater demand for UDP-Gal imposed under inducing conditions by increasing UDP-Gal synthesis in conjunction with transport into the proper luminal compartment.

Once UDP-Gal is translocated into the secretory pathway, the galactose moiety is incorporated into glycoconjugates made in that compartment. These probably include GXMGal, as we previously localized a glycosyltransferase required for GXMGal synthesis to the Golgi compartment (Klutts et al. 2007; Klutts and Doering 2008). Consistent with this finding, GXMGal synthesis is completely abrogated in cells lacking *UGT1* (Moyrand et al. 2007). Paradoxically, capsules of cells lacking *UGT1* are enlarged (Figure 6A), consistent with prior reports (Moyrand et al. 2007). It may be that GXMGal normally participates in capsule polysaccharide organization, so that its absence yields a looser, and therefore more voluminous, structure. Defects in protein glycosylation may also indirectly cause changes in capsule synthesis, for example, via altered enzyme activity or stability.

It is notable that depending on the induction conditions *ugt1*Δ exhibits two distinct capsule phenotypes, being normocapsular in DMEM medium but hypercapsular relative to WT in dilute Sabouraud's broth (Figure 6A). Multiple signaling pathways trigger capsule production in response to distinct environmental or chemical conditions, and we are just beginning to understand the complex interplay between them (Haynes et al. 2011; O'Meara and Alspaugh 2012; Maier et al. 2015). *C. neoformans*, furthermore, is a facultative intracellular pathogen that occupies multiple subenvironments within the host, including the nutrient-limited intracellular and blood stream niches, which we model in vitro with 10% Sabouraud and DMEM, respectively. Capsule thickness is known to vary between organs in infected hosts (Rivera et al. 1998; Garcia-Hermoso et al. 2004); our distinct culture conditions may be similarly inducing changes in both size and organization.

The alterations observed in *ugt1*Δ cells were not isolated to capsule synthesis. Mutant cells have a propensity to aggregate (Fig. 6A); they are also more sensitive to cell wall perturbing reagents (Congo Red, SDS) and less able to tolerate environmental stresses (temperature, H_2O_2) (Figure 6) than WT (Moyrand et al. 2007). These phenotypes suggest defects in cell wall synthesis, again potentially due directly to alterations in component glycans or indirectly due to underglycosylated synthetic machinery. However, since galactose and GalNAc modification of protein-linked glycans in *C.*

neoformans has not been examined to date, these models remain to be tested.

The absence of Ugt1 also resulted in the inability of mutant cells to mate. In *S. cerevisiae*, mating depends on the interaction of two distinct cell surface glycoproteins (Cappellaro et al. 1991), which are five times less active when they are not glycosylated (Cappellaro et al. 1994). Galactosylation of specific determinants may similarly be required for efficient mating to occur in *C. neoformans*. This mechanism also potentially underlies the inability of *S. pombe* mutants deficient in UDP-Gal transport to undergo sexual conjugation during nutritional deprivation (Tanaka et al. 2001).

Finally, we found that *ugt1*Δ cells are rapidly cleared in vitro and in vivo, likely facilitated by the increased recognition and phagocytosis of *ugt1*Δ by macrophages (Figure 8). This result is somewhat surprising, since internalization of hypercapsular mutants is often reduced, attributed to the overall increase in the antiphagocytic capsule. However, if the enlarged capsule of *ugt1*Δ results from poorly organized GXM, rather than overproduction of capsule material, it may not function normally. In this scenario, changes in surface epitope accessibility may result in better recognition by macrophages while the sensitivity profile facilitates clearance. Together, these would result in the avirulence seen both in our inhalational model and in prior studies using intravenous inoculation with pools of mutants (Moyrand et al. 2007).

The pleiotropic defects and general avirulence of cells lacking Ugt1 emphasize the importance of galactose precursor localization to the biology and pathogenicity of *C. neoformans*. Defining the activity of Ugt1 and other NSTs will advance our understanding of glycan biosynthetic pathways, setting the stage for further studies of fundamental glycobiology and cryptococcal pathogenesis.

Supplementary data

Supplementary data for this article is available online at http://glycob.oxfordjournals.org/.

Funding

This work was supported by National Institutes of Health grants GM071007 and AI109623. LXL was partly supported by a Sondra Schlesinger Graduate Fellowship, and National Institute of Health grants F30 AI120339 and T32 GM007200.

Acknowledgements

We thank Matthew Williams for help with the mouse experiments and Wandy Beatty for performing the EM studies. We also thank June Kwon-Chung (NIAID) for cryptococcal strain Jec21, Joe Heitman (Duke University) for strains KN99 and KN433, Jennifer Lodge (Washington University School of Medicine) for plasmid pMH12-T and members of the Doering laboratory for helpful discussions.

Conflict of interest statement

None declared.

Abbreviations

Gal, galactose; Gal_f, galactofuranose; GalNAc, *N*-acetylgalactosamine; GlcA, glucuronic acid; GXM, glucuronoxylomannan; GXMGal, glucuronoxylomannogalactan; G418, geneticin; YPD, yeast extract peptone dextrose; O/N, overnight; MEM, minimal essentials media; SDS, sodium dodecyl sulfate; NAT, nourseothricin; NST, nucleotide sugar transporters; Xyl, xylose; DMEM, Dulbecco's modified Eagle's medium; RNA, ribonucleic acid, WT, wild type.

References

Abeijon C, Mandon EC, Hirschberg CB. 1997. Transporters of nucleotide sugars, nucleotide sulfate and ATP in the Golgi apparatus. *Trends Biochem Sci*. 22:203–207.

Aoki K, Ishida N, Kawakita M. 2001. Substrate recognition by UDP-galactose and CMP-sialic acid transporters. Different sets of transmembrane helices are utilized for the specific recognition of UDP-galactose and CMP-sialic acid. *J Biol Chem*. 276:21555–21561.

Aoki K, Ishida N, Kawakita M. 2003. Substrate recognition by nucleotide sugar transporters: further characterization of substrate recognition regions by analyses of UDP-galactose/CMP-sialic acid transporter chimeras and biochemical analysis of the substrate specificity of parental and chimeric transporters. *J Biol Chem*. 278:22887–22893.

Ashikov A, Routier F, Fuhlrott J, Helmus Y, Wild M, Gerardy-Schahn R, Bakker H. 2005. The human solute carrier gene SLC35B4 encodes a bifunctional nucleotide sugar transporter with specificity for UDP-xylose and UDP-*N*-acetylglucosamine. *J Biol Chem*. 280:27230–27235.

Bakker H, Friedmann I, Oka S, Kawasaki T, Nifant'ev N, Schachner M, Mantei N. 1997. Expression cloning of a cDNA encoding a sulfotransferase involved in the biosynthesis of the HNK-1 carbohydrate epitope. *J Biol Chem*. 272:29942–29946.

Bakker H, Routier F, Oelmann S, Jordi W, Lommen A, Gerardy-Schahn R, Bosch D. 2005. Molecular cloning of two *Arabidopsis* UDP-galactose transporters by complementation of a deficient Chinese hamster ovary cell line. *Glycobiology*. 15:193–201.

Banks IR, Specht CA, Donlin MJ, Gerik KJ, Levitz SM, Lodge JK. 2005. A chitin synthase and its regulator protein are critical for chitosan production and growth of the fungal pathogen *Cryptococcus neoformans*. *Eukaryot Cell*. 4:1902–1912.

Bar-Peled M, Griffith CL, Doering TL. 2001. Functional cloning and characterization of a UDP- glucuronic acid decarboxylase: the pathogenic fungus *Cryptococcus neoformans* elucidates UDP-xylose synthesis. *Proc Natl Acad Sci USA*. 98:12003–12008.

Bar-Peled M, Griffith CL, Ory JJ, Doering TL. 2004. Biosynthesis of UDP-GlcA, a key metabolite for capsular polysaccharide synthesis in the pathogenic fungus *Cryptococcus neoformans*. *Biochem J*. 381:131–136.

Berninsone PM, Hirschberg CB. 2000. Nucleotide sugar transporters of the Golgi apparatus. *Curr Opin Struct Biol*. 10:542–547.

Berninsone P, Hwang HY, Zemtseva I, Horvitz HR, Hirschberg CB. 2001. SQV-7, a protein involved in Caenorhabditis elegans epithelial invagination and early embryogenesis, transports UDP-glucuronic acid, UDP-N-acetylgalactosamine, and UDP-galactose. *Proc Natl Acad Sci USA*. 98:3738–3743.

Beverley SM, Owens KL, Showalter M, Griffith CL, Doering TL, Jones VC, McNeil MR. 2005. Eukaryotic UDP-galactopyranose mutase (*GLF* gene) in microbial and metazoal pathogens. *Eukaryot Cell*. 4:1147–1154.

Botts MR, Hull CM. 2010. Dueling in the lung: How *Cryptococcus* spores race the host for survival. *Curr Opin Microbiol*. 13:437–442.

Caffaro CE, Luhn K, Bakker H, Vestweber D, Samuelson J, Berninsone P, Hirschberg CB. 2008. A single *Caenorhabditis elegans* Golgi apparatus-type transporter of UDP-glucose, UDP-galactose, UDP-*N*-acetylglucosamine, and UDP-*N*-acetylgalactosamine. *Biochemistry*. 47:4337–4344.

Cappellaro C, Baldermann C, Rachel R, Tanner W. 1994. Mating type-specific cell–cell recognition of *Saccharomyces cerevisiae*: cell wall attachment and active sites of a- and alpha-agglutinin. *EMBO J*. 13:4737–4744.

Cappellaro C, Hauser K, Mrsa V, Watzele M, Watzele G, Gruber C, Tanner W. 1991. *Saccharomyces cerevisiae* a- and alpha-agglutinin: Characterization of their molecular interaction. *EMBO J*. 10:4081–4088.

Castle SA, Owuor EA, Thompson SH, Garnsey MR, Klutts JS, Doering TL, Levery SB. 2008. Beta1,2-xylosyltransferase Cxt1p is solely responsible

for xylose incorporation into *Cryptococcus neoformans* glycosphingolipids. *Eukaryot Cell*. 7:1611–1615.

Chang YC, Kwon-Chung KJ. 1994. Complementation of a capsule-deficient mutation of *Cryptococcus neoformans* restores its virulence. *Mol Cell Biol*. 14:4912–4919.

Cherniak R, Valafar H, Morris LC, Valafar F. 1998. *Cryptococcus neoformans* chemotyping by quantitative analysis of 1H nuclear magnetic resonance spectra of glucuronoxylomannans with a computer-simulated artificial neural network. *Clin Diagn Lab Immunol*. 5:146–159.

Chevenet F, Brun C, Banuls AL, Jacq B, Christen R. 2006. TreeDyn: Towards dynamic graphics and annotations for analyses of trees. *BMC Bioinformatics*. 7:439.

Cottrell TR, Griffith CL, Liu H, Nenninger AA, Doering TL. 2007. The pathogenic fungus *Cryptococcus neoformans* expresses two functional GDP-mannose transporters with distinct expression patterns and roles in capsule synthesis. *Eukaryot Cell*. 6:776–785.

Dereeper A, Audic S, Claverie JM, Blanc G. 2010. BLAST-EXPLORER helps you building datasets for phylogenetic analysis. *BMC Evol Biol*. 10:8.

Dereeper A, Guignon V, Blanc G, Audic S, Buffet S, Chevenet F, Dufayard JF, Guindon S, Lefort V, Lescot M et al. 2008. Phylogeny.fr: Robust phylogenetic analysis for the non-specialist. *Nucleic Acids Res*. 36: W465–W469.

Deutscher SL, Hirschberg CB. 1986. Mechanism of galactosylation in the Golgi apparatus. A Chinese hamster ovary cell mutant deficient in translocation of UDP-galactose across Golgi vesicle membranes. *J Biol Chem*. 261:96–100.

Doering TL. 2009. How sweet it is! Cell wall biogenesis and polysaccharide capsule formation in *Cryptococcus neoformans*. *Annu Rev Microbiol*. 63: 223–247.

Edgar RC. 2004. MUSCLE: multiple sequence alignment with high accuracy and high throughput. *Nucleic Acids Res*. 32:1792–1797.

Fu J, Hettler E, Wickes BL. 2006. Split marker transformation increases homologous integration frequency in *Cryptococcus neoformans*. *Fungal Genet Biol*. 43:200–212.

Garcia-Hermoso D, Dromer F, Janbon G. 2004. *Cryptococcus neoformans* capsule structure evolution in vitro and during murine infection. *Infect Immun*. 72:3359–3365.

Gilbert NM, Donlin MJ, Gerik KJ, Specht CA, Djordjevic JT, Wilson CF, Sorrell TC, Lodge JK. 2010. *KRE* genes are required for beta-1,6-glucan synthesis, maintenance of capsule architecture and cell wall protein anchoring in *Cryptococcus neoformans*. *Mol Microbiol*. 76:517–534.

Gilbert NM, Lodge JK, Specht CA. 2011. The cell wall of *Cryptococcus*. In: Heitman J, Kozel TR, Kwon-Chung KJ, Perfect J, Casadevall A, editors. *Cryptococcus From Human Pathogen to Model Yeast* Washington, ASM Press p.67–79.

Griffith CL, Klutts JS, Zhang L, Levery SB, Doering TL. 2004. UDP-glucose dehydrogenase plays multiple roles in the biology of the pathogenic fungus *Cryptococcus neoformans*. *J Biol Chem*. 279:51669–51676.

Guindon S, Gascuel O. 2003. A simple, fast, and accurate algorithm to estimate large phylogenies by maximum likelihood. *Syst Biol*. 52:696–704.

Hadley B, Maggioni A, Ashikov A, Day CJ, Haselhorst T, Tiralongo J. 2014. Structure and function of nucleotide sugar transporters: Current progress. *Comput Struct Biotechnol J*. 10:23–32.

Haynes BC, Skowyra ML, Spencer SJ, Gish SR, Williams M, Held EP, Brent MR, Doering TL. 2011. Toward an integrated model of capsule regulation in *Cryptococcus neoformans*. *PLoS Pathog*. 7:e1002411.

Heise N, Gutierrez AL, Mattos KA, Jones C, Wait R, Previato JO, Mendonca-Previato L. 2002. Molecular analysis of a novel family of complex glycoinositolphosphoryl ceramides from *Cryptococcus neoformans*: Structural differences between encapsulated and acapsular yeast forms. *Glycobiology*. 12:409–420.

Heiss C, Klutts JS, Wang Z, Doering TL, Azadi P. 2009. The structure of *Cryptococcus neoformans* galactoxylomannan contains beta-D-glucuronic acid. *Carbohydr Res*. 344:915–920.

Heiss C, Skowyra ML, Liu H, Klutts JS, Wang Z, Williams M, Srikanta D, Beverley SM, Azadi P, Doering TL. 2013. Unusual galactofuranose modification of a capsule polysaccharide in the pathogenic yeast *Cryptococcus neoformans*. *J Biol Chem*. 288:10994–11003.

Klutts JS, Doering TL. 2008. Cryptococcal xylosyltransferase 1 (Cxt1p) from *Cryptococcus neoformans* plays a direct role in the synthesis of capsule polysaccharides. *J Biol Chem*. 283:14327–14334.

Klutts JS, Levery SB, Doering TL. 2007. A beta-1,2-xylosyltransferase from *Cryptococcus neoformans* defines a new family of glycosyltransferases. *J Biol Chem*. 282:17890–17899.

Kruse J, Mailhammer R, Wernecke H, Faissner A, Sommer I, Goridis C, Schachner M. 1984. Neural cell adhesion molecules and myelin-associated glycoprotein share a common carbohydrate moiety recognized by monoclonal antibodies L2 and HNK-1. *Nature*. 311: 153–155.

Kumar P, Yang M, Haynes BC, Skowyra ML, Doering TL. 2011. Emerging themes in cryptococcal capsule synthesis. *Curr Opin Struct Biol*. 21: 597–602.

Kwon-Chung KJ, Edman JC, Wickes BL. 1992. Genetic association of mating types and virulence in *Cryptococcus neoformans*. *Infect Immun*. 60: 602–605.

Kwon-Chung KJ, Varma A. 2006. Do major species concepts support one, two or more species within *Cryptococcus neoformans*? *FEMS Yeast Res*. 6:574–587.

Kwon-Chung KJ, Wickes BL, Stockman L, Roberts GD, Ellis D, Howard DH. 1992. Virulence, serotype, and molecular characteristics of environmental strains of *Cryptococcus neoformans var. gattii*. *Infect Immun*. 60: 1869–1874.

Maier EJ, Haynes BC, Gish SR, Wang ZA, Skowyra ML, Marulli AL, Doering TL, Brent MR. 2015. Model-driven mapping of transcriptional networks reveals the circuitry and dynamics of virulence regulation. *Genome Res*. 25:690–700.

Martinez-Duncker I, Mollicone R, Codogno P, Oriol R. 2003. The nucleotide-sugar transporter family: a phylogenetic approach. *Biochimie*. 85:245–260.

Maszczak-Seneczko D, Sosicka P, Majkowski M, Olczak T, Olczak M. 2012. UDP-*N*-acetylglucosamine transporter and UDP-galactose transporter form heterologous complexes in the Golgi membrane. *FEBS Lett*. 586: 4082–4087.

Moyrand F, Fontaine T, Janbon G. 2007. Systematic capsule gene disruption reveals the central role of galactose metabolism on *Cryptococcus neoformans* virulence. *Mol Microbiol*. 64:771–781.

Moyrand F, Lafontaine I, Fontaine T, Janbon G. 2008. *UGE1* and *UGE2* regulate the UDP-glucose/UDP-galactose equilibrium in *Cryptococcus neoformans*. *Eukaryot Cell*. 7:2069–2077.

Nielsen K, Cox GM, Litvintseva AP, Mylonakis E, Malliaris SD, Benjamin DK Jr, Giles SS, Mitchell TG, Casadevall A, Perfect JR et al. 2005. *Cryptococcus neoformans {alpha}* strains preferentially disseminate to the central nervous system during coinfection. *Infect Immun*. 73:4922–4933.

Nielsen K, Cox GM, Wang P, Toffaletti DL, Perfect JR, Heitman J. 2003. Sexual cycle of *Cryptococcus neoformans var. grubii* and virulence of congenic a and alpha isolates. *Infect Immun*. 71:4831–4841.

Norambuena L, Marchant L, Berninsone P, Hirschberg CB, Silva H, Orellana A. 2002. Transport of UDP-galactose in plants. Identification and functional characterization of AtUTr1, an *Arabidopsis thaliana* UDP-galactos/UDP-glucose transporter. *J Biol Chem*. 277:32923–32929.

O'Meara TR, Alspaugh JA. 2012. The *Cryptococcus neoformans* capsule: A sword and a shield. *Clin Microbiol Rev*. 25:387–408.

Oelmann S, Stanley P, Gerardy-Schahn R. 2001. Point mutations identified in Lec8 Chinese hamster ovary glycosylation mutants that inactivate both the UDP-galactose and CMP-sialic acid transporters. *J Biol Chem*. 276: 26291–26300.

Olson GM, Fox DS, Wang P, Alspaugh JA, Buchanan KL. 2007. Role of protein O-mannosyltransferase Pmt4 in the morphogenesis and virulence of *Cryptococcus neoformans*. *Eukaryot Cell*. 6:222–234.

Park JN, Lee DJ, Kwon O, Oh DB, Bahn YS, Kang HA. 2012. Unraveling unique structure and biosynthesis pathway of N-linked glycans in human fungal pathogen *Cryptococcus neoformans* by glycomics analysis. *J Biol Chem*. 287:19501–19515.

Park BJ, Wannemuehler KA, Marston BJ, Govender N, Pappas PG, Chiller TM. 2009. Estimation of the current global burden of cryptococcal meningitis among persons living with HIV/AIDS. *Aids*. 23:525–530.

Reese AJ, Doering TL. 2003. Cell wall alpha-1,3-glucan is required to anchor the *Cryptococcus neoformans* capsule. *Mol Microbiol*. 50:1401–1409.

Reese AJ, Yoneda A, Breger JA, Beauvais A, Liu H, Griffith CL, Bose I, Kim MJ, Skau C, Yang S et al. 2007. Loss of cell wall alpha(1–3) glucan affects *Cryptococcus neoformans* from ultrastructure to virulence. *Mol Microbiol*. 63:1385–1398.

Reilly MC, Aoki K, Wang ZA, Skowyra ML, Williams M, Tiemeyer M, Doering TL. 2011. A xylosylphosphotransferase of *Cryptococcus neoformans* acts in protein O-glycan synthesis. *J Biol Chem*. 286:26888–26899.

Rittershaus PC, Kechichian TB, Allegood JC, Merrill AH Jr, Hennig M, Luberto C, Del Poeta M. 2006. Glucosylceramide synthase is an essential regulator of pathogenicity of *Cryptococcus neoformans*. *J Clin Invest*. 116:1651–1659.

Rivera J, Feldmesser M, Cammer M, Casadevall A. 1998. Organ-dependent variation of capsule thickness in *Cryptococcus neoformans* during experimental murine infection. *Infect Immun*. 66:5027–5030.

Segawa H, Kawakita M, Ishida N. 2002. Human and *Drosophila* UDP-galactose transporters transport UDP-*N*-acetylgalactosamine in addition to UDP-galactose. *Eur J Biochem*. 269:128–138.

Segawa H, Soares RP, Kawakita M, Beverley SM, Turco SJ. 2005. Reconstitution of GDP-mannose transport activity with purified *Leishmania* LPG2 protein in liposomes. *J Biol Chem*. 280:2028–2035.

Srikanta D, Yang M, Williams M, Doering TL. 2011. A sensitive high-throughput assay for evaluating host–pathogen interactions in *Cryptococcus neoformans* infection. *PloS One*. 6:e22773.

Tanaka N, Konomi M, Osumi M, Takegawa K. 2001. Characterization of a *Schizosaccharomyces pombe* mutant deficient in UDP-galactose transport activity. *Yeast*. 18:903–914.

Terayama K, Oka S, Seiki T, Miki Y, Nakamura A, Kozutsumi Y, Takio K, Kawasaki T. 1997. Cloning and functional expression of a novel glucuronyltransferase involved in the biosynthesis of the carbohydrate epitope HNK-1. *Proc Natl Acad Sci USA*. 94:6093–6098.

Varki A, Esko JD, Colley KJ. 2009. Cellular Organization of Glycosylation. In: Varki A, Cummings RD, Esko JD, Freeze HH, Stanley P, Bertozzi CR, Hart GW, Etzler ME, editors. *Essentials of Glycobiology* (p. 37-46). Cold Spring Harbor, NY, Cold Spring Harbor Laboratory Press.

Vincent VL, Klig LS. 1995. Unusual effect of *myo*-inositol on phospholipid biosynthesis in *Cryptococcus neoformans*. *Microbiology*. 141(Pt 8): 1829–1837.

Voelz K, May RC. 2010. Cryptococcal interactions with the host immune system. *Eukaryot Cell*. 9:835–846.

Wang ZA, Griffith CL, Skowyra ML, Salinas N, Williams M, Maier EJ, Gish SR, Liu H, Brent MR, Doering TL. 2014. *Cryptococcus neoformans* dual GDP-mannose transporters and their role in biology and virulence. *Eukaryot Cell*. 13:832–842.

Waterhouse AM, Procter JB, Martin DM, Clamp M, Barton GJ. 2009. Jalview Version 2—a multiple sequence alignment editor and analysis workbench. *Bioinformatics*. 25:1189–1191.

Wills EA, Roberts IS, Del Poeta M, Rivera J, Casadevall A, Cox GM, Perfect JR. 2001. Identification and characterization of the *Cryptococcus neoformans* phosphomannose isomerase-encoding gene, *MAN1*, and its impact on pathogenicity. *Mol Microbiol*. 40:610–620.

Wohlschlager T, Buser R, Skowyra ML, Haynes BC, Henrissat B, Doering TL, Kunzler M, Aebi M. 2013. Identification of the galactosyltransferase of *Cryptococcus neoformans* involved in the biosynthesis of basidiomycete-type glycosylinositolphosphoceramide. *Glycobiology*. 23: 1210–1219.

Yoneda A, Doering TL. 2006. A eukaryotic capsular polysaccharide is synthesized intracellularly and secreted via exocytosis. *Mol Biol Cell*. 17: 5131–5140.

Zaragoza O, Casadevall A. 2004. Experimental modulation of capsule size in *Cryptococcus neoformans*. *Biol Proced Online*. 6:10–15.